Magnetic Moments and Electron Spin Resonance Spectra of Some Iron–Sulphur–Molybdenum and –Tungsten Cubane-like Cluster Dimers

By **George Christou, David Collison, C.David Garner, Stephen R. Acott,** and **Frank E. Mabbs,*** Chemistry Department, University of Manchester, Manchester M13 9PL
Vasili Petrouleas, Greek Atomic Energy Commission, Nuclear Research Centre Demokritos, Aghia Paraskevi, Attiki, Greece

The variation of the effective magnetic moment, $\bar{\mu}_m$, with temperature in the range 1.9—300 K, and with applied magnetic field (1.25—20.0 kG), is reported for $[NEt_4]_3[Fe_6M_2S_8(SPh)_6(OMe)_3]$ [M = Mo (1) or W (2)], $[NBu^n_4]_3[Fe_6Mo_2S_8(SPh)_9]$ (3), and $[NEt_4]_3[Fe_6W_2S_8(SEt)_9]$ (4). The e.s.r. spectra at 4.2 K for powders of (2), (3), and (4), and a frozen glass in MeCN for (2) are also reported. An interpretation of these data is presented in terms of antiferromagnetic spin coupling between two Fe^{II} ions and an Fe^{III} ion within a Fe_3MS_4 sub-unit, with an additional much weaker couping between the sub-units.

MANY compounds have now been prepared which consist of a pair of $Fe_3MS_4(SR)_3$ units, each with a cubane-like core, bridged by other groups. Several basic anionic types have been identified which include $[Fe_6M_2S_8(SR)_9]^{3-}$, [1-9] $[Fe_6M_2S_8(SR)_6(OMe)_3]^{3-}$, [9-11] $[Fe_6M_2S_9(SR)_8]^{3-}$, [8-12] $[Fe_7Mo_2S_8(SR)_{12}]^{3-/4-}$, [7,8] and $[Fe_6M_2S_8(SEt)_6\{2,3\text{-}(OH)_2\text{-}1,4\text{-}Pr^n_2C_6H_2\}_2]^{4-}$, [13] where M = Mo or W. The extended *X*-ray absorption fine structures (EXAFS) of the molybdenum-containing compounds are similar to those of the FeMo protein from *Azotobacter vinelandii* and *Clostridium pasteuranium* [14] suggesting that these cluster compounds may be suitable synthetic analogues of these nitrogenase proteins. The proton magnetic resonance,[8,9] Mössbauer,[5,8,11] and electrochemical [8,11] properties of the above cube-cluster dimers have been reported in some detail. However, reports of the magnetic susceptibilities [8] and e.s.r.[12] behaviour of these compounds are very sparse. The most detailed report of experimental magnetic susceptibility data and its interpretation is our preliminary report [15] on the compounds $[NEt_4]_3[Fe_6M_2S_8(SPh)_6(OMe)_3]$ (M = Mo or W).

The descriptions of the electronic structures of these mixed metal cube-cluster dimers, and indeed the formally simpler iron–sulphur cluster, which readily allow detailed interpretation of magnetic and e.s.r. data, is at present not very good. As part of a programme to improve our understanding we now wish to report the bulk magnetic susceptibilities and e.s.r. spectra of a number of structurally characterised molybdenum- and tungsten-containing cube-cluster dimer compounds. Three of the compounds studied, $[NEt_4]_3[Fe_6W_2S_8(SEt)_9]$ and $[NEt_4]_3[Fe_6M_2S_8(SPh)_6(OMe)_3]$ (M = Mo or W), crystallise in the hexagonal space group $P6_3/m$ with the cubane-like cluster dimer located on a site of C_{3h} symmetry.[3,10] The other compound, $[NBu^n_4]_3[Fe_6Mo_2S_8(SPh)_9]$, crystallises in the monoclinic space group C_c, but the discrete anions still approximate very closely to C_{3h} symmetry.[1] Thus the cubane-like cluster dimer, and also each cubane-like sub-unit, can be assumed to be axially symmetric. The interpretation of the magnetic susceptibility data is based on the model already outlined,[15] whilst e.s.r. data utilise the computer simulation method described in the preceding paper.

EXPERIMENTAL

Analytically pure samples of $[NEt_4]_3[Fe_6M_2S_8(SPh)_6(OMe)_3]$ [M = Mo (1) or W (2)], $[NBu^n_4]_3[Fe_6Mo_2S_8(SPh)_9]$ (3), and $[NEt_4]_3[Fe_6W_2S_8(SEt)_9]$ (4) were prepared as described previously.[9]

Magnetic Susceptibility Measurements.—These were made using a PAR vibrating sample magnetometer (model 155) equipped with a variable-temperature cryostat (model 153) and a Varian model V-7800 magnet. The sample holder and the lowest end of the vibrating rod were modified so that the sample volume was increased to a maximum, whilst the signal from the empty sample holder and the *z*-position dependence were minimised. Temperatures in the range 1.6—40 K were measured with a Johnson-Matthey gold (0.03% Fe) *versus* silver thermocouple attached to the sample holder (this thermocouple is weakly diamagnetic). Higher temperatures were measured with the copper-constantan thermocouple provided with the cryostat. Temperature calibration was achieved by using a germanium resistor and the paramagnetic standards [16] $Hg[Co(NCS)_4]$ and $[Me_2NH(CH_2)_2NHMe_2][CuCl_4]$.

Estimated errors in the measurements are as follows. (*i*) Temperature: systematic deviations of the temperature calibration and fluctuations during measurement were estimated to be within ±0.5 in the range 1.6—15 K, ±0.1 in the range 15—40 K, and ±0.3 K at higher temperatures.

(*ii*) Molar susceptibility: the estimated errors are approximately ±0.3% of the value at each temperature. Temperature induced errors, particularly at low temperatures, should be added to this.

Electron Spin Resonance Spectra.—First derivative e.s.r. spectra at *X*-band frequencies were obtained using a Varian E112 spectrometer system. Sample temperatures in the range 4.2—300 K were obtained using an Oxford Instruments ESR 9 continuous flow cryostat coupled to an Oxford Instruments Harwell DT temperature controller. The temperature of the coolant gas stream was measured with a gold(0.03% Fe)–chromel thermocouple. Samples were loaded into 2 mm (outside diameter) silica tubes with a cupped top which could be sealed with a septum cap. Powders were packed under a stream of dry purified dinitrogen which was also used as the atmosphere in the sample tube. Solution spectra were obtained using dry degassed methyl cyanide. We found that the spectra were reproducible between different preparations of the same compound, and also quite different from those obtained upon exposure of the samples to air.

RESULTS

The temperature dependence of the effective magnetic moments for compounds (1)—(4) are given in Tables 1—4 and Figures 1—4 respectively. The magnetic field dependences of the effective magnetic moments at low temperature

TABLE 1

Variation of effective magnetic moment, $\bar{\mu}_m$, with temperature for $[NEt_4]_3[Fe_6Mo_2S_8(SPh)_6(OMe)_3]$ (1)

T/K	H/kG	$\bar{\mu}_m$/B.M.
298.81	20.0	5.74
272.62	15.0	5.73
200.32	15.0	5.69
140.23	15.0	5.69
94.84	10.0	5.63
64.41	10.0	5.60
44.68	10.0	5.53
34.98	10.0	5.52
27.65	10.0	5.46
22.73	5.0	5.41
17.28	5.0	5.39
16.08	5.0	5.38
12.67	5.0	5.32
11.22	5.0	5.30
8.61	5.0	5.22
7.60	5.0	5.18
7.60	2.50	5.18
5.20	2.50	4.91

are in Tables 5—8. The e.s.r. spectra for powdered samples of compounds (3) and (4) are in Figure 5, whilst those for compound (2) are in Figure 6 (powdered sample) and Figure 7 (frozen solution).

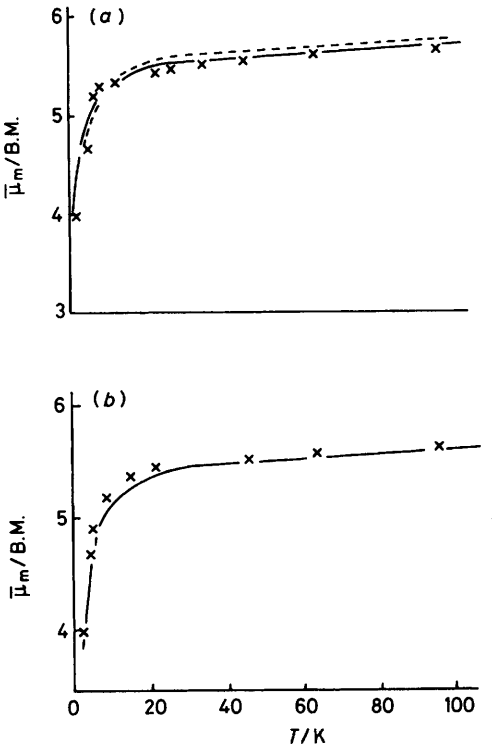

FIGURE 1 Experimental (×) and calculated $\bar{\mu}_m$ *versus* temperature for $[NEt_4]_3[Fe_6Mo_2S_8(SPh)_6(OMe)_3]$ (1). (*a*) Model (*ii*): (——) $J = -120$ cm^{-1}, $\alpha = 2.975$, $\beta = -0.0004$, $g_{\parallel} = 1.92$, $g_{\perp} = 1.89$, $D = 3.0$ cm^{-1}; (– – – –) $J = -60$ cm^{-1}, $\alpha = 2.956$, $\beta = 0.0$, $g_{\parallel} = 1.93$, $g_{\perp} = 1.90$, $D = 1.7$ cm^{-1}; (*b*) model (*iii*): (——) $J = -120$ cm^{-1}, $\alpha = 0.6287$, $\beta = -0.0006$, $g_{\parallel} = 2.55$, $g_{\perp} = 2.25$, $D = 2.0$ cm^{-1}

TABLE 2

Variation of $\bar{\mu}_m$ with temperature for $[NEt_4]_3[Fe_6W_2S_8(SPh)_6(OMe)_3]$ (2)

T/K	H/kG	$\bar{\mu}_m$/B.M.
289.75	20.0	5.81
289.75	10.0	5.80
247.75	10.0	5.81
217.10	10.0	5.80
213.49	10.0	5.80
149.45	10.0	5.74
98.64	10.0	5.67
80.23	10.0	5.65
63.02	10.0	5.65
51.92	10.0	5.63
47.05	10.0	5.58
41.92	10.0	5.55
41.92	5.0	5.56
41.61	5.0	5.55
38.29	5.0	5.55
32.85	5.0	5.59
27.70	5.0	5.54
22.37	5.0	5.47
15.72	2.5	5.33
12.35	2.5	5.27
6.83	2.5	5.04
5.45	2.5	4.77

Theoretical Treatment of the Data.—Although there have been a number of attempts to describe the electronic structures of iron–sulphur cluster compounds using LCAO (linear combination of atomic orbitals) molecular orbital treatments [17-27] the results have so far been confined to descriptions of the ground states. In no case has the quantitative prediction of excited states necessary for the calculation of the variation of magnetic moments with temperature and applied magnetic field been made. Similarly, a

TABLE 3

Variation of $\bar{\mu}_m$ with temperature for $[NBu^n_4]_3[Fe_6Mo_2S_8(SPh)_9]$ (3)

T/K	H/kG	$\bar{\mu}_m$/B.M.	Sample
297.2	10.0	5.71	A
292.6	10.0	5.68	B
270.8	10.0	5.69	A
199.2	10.0	5.67	A
150.0	10.0	5.69	A
136.5	10.0	5.64	B
109.6	10.0	5.67	A
96.4	10.0	5.64	B
76.7	10.0	5.67	A
71.9	10.0	5.66	B
55.5	10.0	5.68	A
37.7	10.0	5.65	B
37.5	10.0	5.65	A
36.0	10.0	5.65	B
32.9	5.0	5.67	B
31.5	5.0	5.63	B
28.8	10.0	5.60	B
27.6	5.0	5.62	B
26.5	5.0	5.66	A
25.3	5.0	5.62	B
21.6	5.0	5.62	B
16.9	10.0	5.68	A
15.5	5.0	5.66	B
13.5	5.0	5.71	A
12.9	5.0	5.72	B
12.42	2.5	5.75	B
10.47	2.5	5.80	B
10.08	2.5	5.79	B
8.35	2.5	5.83	B
7.46	2.5	5.84	B
7.20	2.5	5.86	B
5.63	2.5	5.88	B
4.18	2.5	5.90	A
1.95	2.5	5.64	A

TABLE 4

Variation of $\bar{\mu}_m$ with temperature for $[NEt_4]_3[Fe_6W_2S_8(SEt)_9]$ (4)

T/K	H/kG	$\bar{\mu}_m$/B.M.
294.93	20.0	5.75
294.93	10.0	5.74
260.33	10.0	5.72
218.90	10.0	5.66
188.27	10.0	5.62
149.56	10.0	5.57
114.59	10.0	5.60
110.83	10.0	5.49
89.77	10.0	5.54
66.32	10.0	5.52
49.79	10.0	5.46
39.55	10.0	5.41
39.35	5.0	5.43
30.51	5.0	5.40
25.61	5.0	5.36
18.05	2.5	5.36
14.99	2.5	5.36
12.00	2.5	5.36
8.37	2.5	5.33
6.48	2.5	5.24
5.23	2.5	5.18

SCF-Xα-SW (self consistent field Xα-scattered wave) calculation has been reported [28] for the system $[Fe_4S_4(SCH_3)_4]^{2-}$ wherein only the ground state electronic structure was described. This detailed ground-state description has however recently been disputed.[27] It has been shown [29] that it is possible approximately to relate spin state splittings from Xα-SW calculations to the exchange coupling parameter,

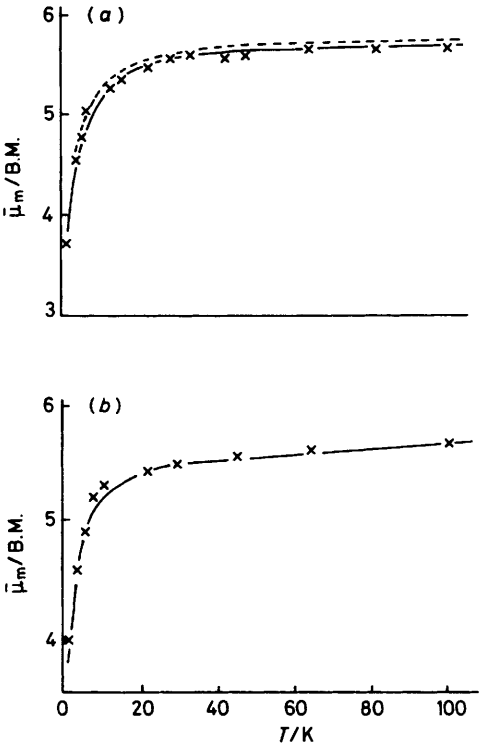

FIGURE 2 Experimental (×) and calculated $\bar{\mu}_m$ *versus* temperature for $[NEt_4]_3[Fe_6W_2S_8(SPh)_6(OMe)_3]$ (2). (*a*) Model (*ii*): (——) $J = -120$ cm^{-1}, $\alpha = 2.970$, $\beta = -0.0006$, $g_{\parallel} = 1.94$, $g_{\perp} = 1.91$, $D = 3.0$ cm^{-1}; (– – –) $J = -60$ cm^{-1}, $\alpha = 2.950$, $\beta = 0.0$, $g_{\parallel} = 1.95$, $g_{\perp} = 1.92$, $D = 1.73$ cm^{-1}; (*b*) model (*iii*): (——) $J = -120$ cm^{-1}, $\alpha = 0.6284$, $\beta = 0.001$, $g_{\parallel} = 2.56$, $g_{\perp} = 2.26$, $D = 2.0$ cm^{-1}

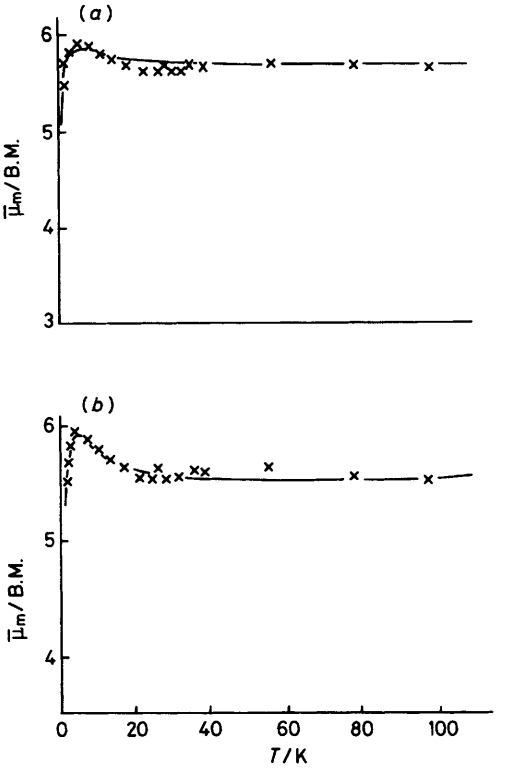

FIGURE 3 Experimental (×) and calculated $\bar{\mu}_m$ *versus* temperature for $[NBu^n_4]_3[Fe_6Mo_2S_8(SPh)_8]$ (3). (*a*) Model (*ii*): (——) $J = -120$ cm^{-1}, $\alpha = 2.978$, $\beta = -0.0051$, $g_{\parallel} = 1.90$, $g_{\perp} = 1.87$, $D = 3.0$ cm^{-1}; (*b*) model (*iii*): (——) $J = -120$ cm^{-1}, $\alpha = 0.6285$, $\beta = -0.009$, $g_{\parallel} = 2.12$, $g_{\perp} = 2.42$, $D = 1.25$ cm^{-1}

J_{ab}, in the spin-Hamiltonian $\mathcal{H}_{ex} = -2\sum_{pairs} J_{ab}\mathbf{S}_a.\mathbf{S}_b$, which is used to describe the magnetic properties of clusters where individual centres have no orbital angular momentum. This technique has been applied to calculation [30] of the exchange parameter in the idealised systems $[Fe_2S_2(SH)_4]^{2-/3-}$. However, at present the only method employed to interpret quantitatively the variation of the magnetic moments of clusters of the type $[Fe_4S_4(SR)_4]^{n-}$,[31-38] and $[Fe_6M_2S_8(SPh)_6(OMe)_3]$,[8-15] is that of calculating the final

TABLE 5

Variation of $\bar{\mu}_m$ with applied magnetic field, H, for $[NEt_4]_3[Fe_6Mo_2S_8(SPh)_6(OMe)_3]$ (1)

			$\bar{\mu}_m$/B.M. (Calculated)		
T/K	H/kG	$\bar{\mu}_m$/B.M. (Found)	model (*ii*) [a]	model (*iii*) [b]	model (*iii*) [c]
4.18	1.25	4.66	4.74	4.64	4.69
	2.5	4.66	4.74	4.64	4.69
	5.0	4.65	4.73	4.64	4.68
	7.5	4.64	4.72	4.63	4.67
	10.0	4.63	4.70	4.62	4.66
	15.0	4.63	4.64	4.60	4.63
	20.0	4.57	4.57	4.55	4.59
1.96	1.25	3.93	3.92	3.92	3.91
	2.5	3.92	3.91	3.91	3.90
	5.0	3.90	3.89	3.90	3.89
	7.5	3.87	3.85	3.88	3.87
	10.0	3.85	3.80	3.86	3.85
	15.0	3.80	3.68	3.79	3.79
	20.0	3.72	3.56	3.71	3.71

Parameters as in Table 9: [a] model (*ii*) (1); [b] model (*iii*) (1a); [c] model (*iii*) (1b).

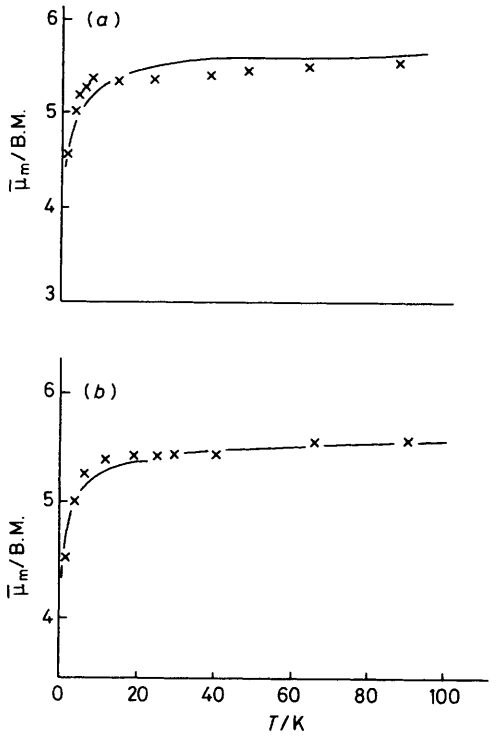

FIGURE 4 Experimental (×) and calculated $\bar{\mu}_m$ *versus* temperature for $[NEt_4]_3[Fe_6W_2S_8(SEt)_9]$ (4). (*a*) Model (*ii*): (——) $J = -120$ cm^{-1}, $\alpha = 2.975$, $\beta = -0.0005$, $g_{\parallel} = 1.92$, $g_{\perp} = 1.89$, $D = -5.0$ cm^{-1}; (*b*) model (*iii*): (——) $J = -120$ cm^{-1}, $\alpha = 0.6288$, $\beta = -0.0022$, $g_{\parallel} = 2.12$, $g_{\perp} = 2.42$, $D = 4.0$ cm^{-1}, $\theta = +0.5°$

spin states of the system *via* spin coupling between metal centres which are formally in integral oxidation states.

We have previously reported [15] an approach to the calculation of the magnetic data for compounds (1) and (2). In that report the cube-cluster dimers were assumed to contain two independent cubane-like Fe_3MS_4 sub-units. The metal atoms in each of these sub-units may be associated with eleven positive charges arising from one of four possible combinations of formal integral oxidation states: (*i*) $3 \times Fe^{III} + M^{II}$; (*ii*) $2 \times Fe^{III} + Fe^{II} + M^{III}$; (*iii*) $Fe^{III} + 2 \times Fe^{II} + M^{IV}$; (*iv*) $3 \times Fe^{II} + M^{V}$. However, Mössbauer data suggest that the iron atoms have on average a non-integral oxidation state. Thus models (*ii*) and (*iii*) appear to afford the most likely starting points for a description of the magnetic properties assuming spin coupling

TABLE 6

Variation of $\bar{\mu}_m$ with applied magnetic field, H, for $[NEt_4]_3[Fe_6W_2S_8(SPh)_6(OMe)_3]$ (2)

			$\bar{\mu}_m$/B.M. (Calculated)		
T/K	H/kG	$\bar{\mu}_m$/B.M. (Found)	model (*ii*) [a]	model (*iii*) [b]	model (*iii*) [c]
4.18	1.25	4.53	4.59	4.53	4.54
	2.5	4.55	4.59	4.53	4.54
	5.0	4.51	4.59	4.52	4.53
	7.5	4.50	4.57	4.52	4.53
	10.0	4.49	4.55	4.51	4.52
	15.0	4.48	4.50	4.49	4.49
	20.0	4.42	4.44	4.45	4.46
2.20	1.25	3.91	3.87	3.91	3.88
	2.5	3.92	3.86	3.90	3.82
	5.0	3.89	3.84	3.89	3.87
	7.5	3.87	3.81	3.88	3.86
	10.0	3.84	3.77	3.87	3.84
	15.0	3.78	3.66	3.82	3.80
	20.0	3.68	3.56	3.76	3.74

Parameters as in Table 9: [a] model (*ii*) (2); [b] model (*iii*) (2a); [c] model (*iii*) (2b).

TABLE 7

Variation of $\bar{\mu}_m$ with applied magnetic field, H, for $[NBu^n_4]_3[Fe_6Mo_2S_8(SPh)_9]$ (3)

			$\bar{\mu}_m$/B.M. (Calculated)	
T/K	H/kG	$\bar{\mu}_m$/B.M. (Found)	model (*ii*) [a]	model (*iii*) [b]
4.18	1.25	5.95	5.93	5.88
	2.5	5.90	5.92	5.87
	5.0	5.84	5.89	5.85
	7.5	5.81	5.84	5.82
	10.0	5.77	5.77	5.77
	15.0	5.68	5.59	5.66
	20.0	5.50	5.39	5.51
1.95	1.25	5.70	5.76	5.71
	2.5	5.64	5.72	5.68
	5.0	5.54	5.57	5.60
	7.5	5.40	5.35	5.47
	10.0	5.24	5.11	5.31
	15.0	4.94	4.67	4.97
	20.0	4.54	4.31	4.65

Parameters as in Table 9: [a] model (*ii*) (3); [b] model (*iii*) (3).

TABLE 8

Variation of $\bar{\mu}_m$ with applied magnetic field, H, for $[NEt_4]_3[Fe_6W_2S_8(SEt)_9]$ (4)

			$\bar{\mu}_m$/B.M. (Calculated)	
T/K	H/kG	$\bar{\mu}_m$/B.M. (Found)	model (*ii*) [a]	model (*iii*) [b]
4.18	1.25	5.04	4.99	4.90
	2.5	4.97	4.98	4.89
	5.0	4.90	4.96	4.88
	7.5	4.85	4.93	4.86
	10.0	4.81	4.89	4.82
	15.0	4.74	4.77	4.74
	20.0	4.62	4.63	4.64
2.01	1.25	4.53	4.59	4.56
	2.5	4.50	4.58	4.54
	5.0	4.40	4.55	4.45
	7.5	4.29	4.47	4.36
	10.0	4.19	4.34	4.23
	15.0	3.96	4.00	3.96
	20.0	3.74	3.68	3.69

Parameters as in Table 9: [a] model (*ii*) (4); [b] model (*iii*) (4).

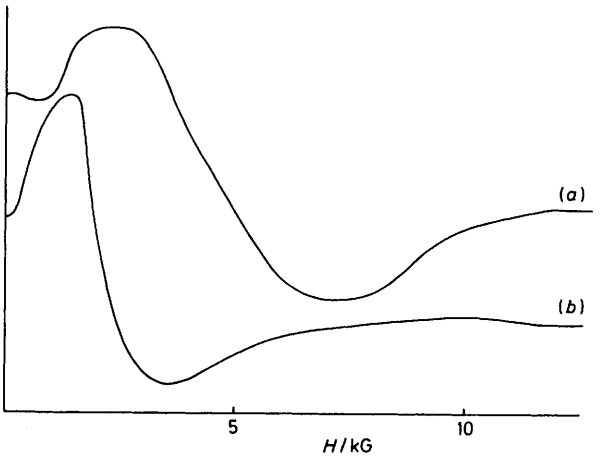

FIGURE 5 Powder e.s.r. spectra at 4.2 K of (*a*) $[NBu^n_4]_3[Fe_6Mo_2S_8(SPh)_9]$ (3) and (*b*) $[NEt_4]_3[Fe_6W_2S_8(SEt)_9]$ (4)

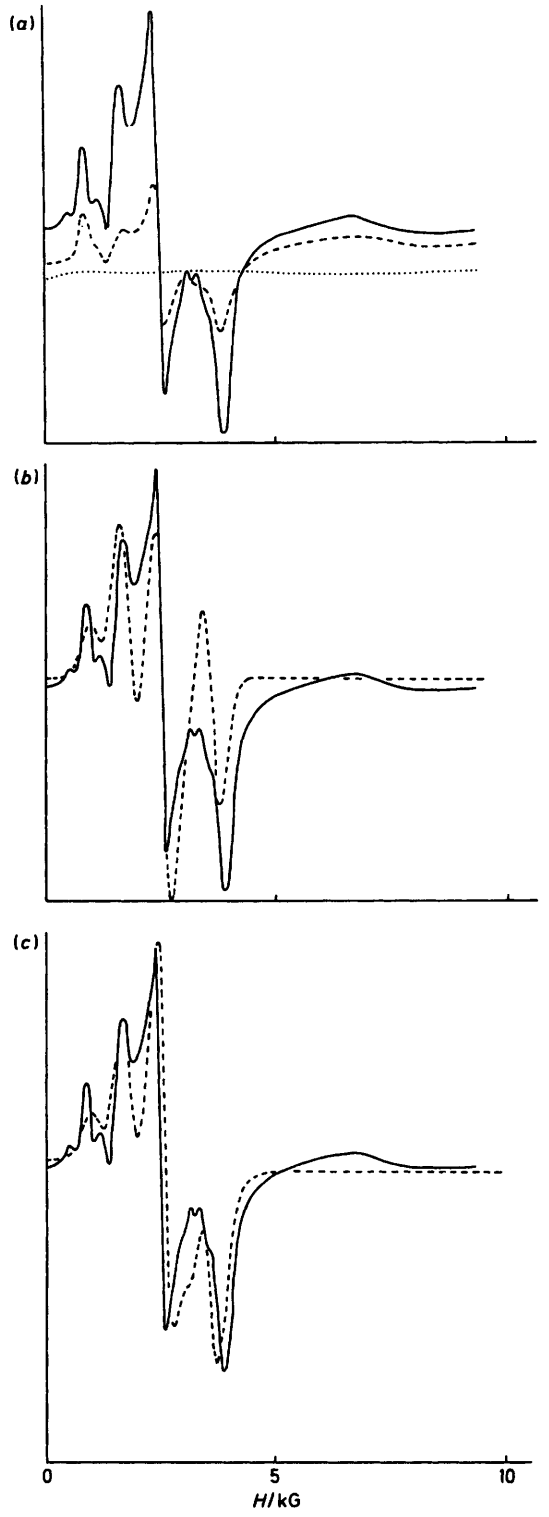

FIGURE 6 Powder e.s.r. spectra of $[NEt_4]_3[Fe_6W_3S_8(SPh)_6(OMe)_3]$ (2), $\nu = 9.328$ GHz. (*a*) Experimental at 4.2 (——), 10 (– – – –), 25 K (· · · ·); (*b*) experimental at 4.2 K (——), calculated for model (*iii*) (– – – –) with $g_{\parallel} = g_{\perp} = 2.25$, $D = 2.0$ cm^{-1}, $\beta J = -0.03$ cm^{-1} $E_a(S' = \frac{1}{2}) = E_b(S' = \frac{1}{2}) = 0.0$ cm^{-1}, $E_a(S' = \frac{3}{2}) = E_b(S' = \frac{3}{2}) = 4.0$ cm^{-1}, $\delta H = 10$ G, $\Delta H = 200$ G, $d\theta = 3°$. $S' = \frac{3}{2}$ coupled with $S' = \frac{1}{2}$ only. Linewidths $w_{\parallel} = 300$, $w_{\perp} = 450$ G; (*c*) experimental at 4.2 K (——); calculated for model (*iii*) (——) with $g_{\parallel} = g_{\perp} = 2.25$, $D = 2.0$ cm^{-1}, $\beta J = -0.03$ cm^{-1} $E_a(S' = \frac{1}{2}) = E_b(S' = \frac{1}{2}) = 0.0$ cm^{-1}, $E_a(S' = \frac{3}{2}) = E_b(S' = \frac{3}{2}) = 4.0$ cm^{-1}, $\delta H = 10$ G, $\Delta H = 200$ G, $d\theta = 3°$. Linewidths for (i) $S'_a = \frac{3}{2}$ coupled with $S'_b = \frac{1}{2}$ (and *vice versa*), $w_{\parallel} = 300$, $w_{\perp} = 450$ G; (ii) $S'_a = \frac{1}{2}$ coupled with $S'_b = \frac{1}{2}$, $w_{\parallel} = w_{\perp} = 1\,000$ G; (iii) $S'_a = \frac{3}{2}$ coupled with $S'_b = \frac{3}{2}$, $w_{\parallel} = w_{\perp} = 2\,000$ G

within a sub-unit. Proton n.m.r. data [9] suggest that there is greater paramagnetism associated with the terminal compared to the bridging ligands. This interpretation was used to support the assumption that any unpaired electrons formally associated with the metal M are in fact paired through a combination of distorted octahedral geometry about these atoms and electronic exchange interactions across the bridging region.[15]

Based on the magnetic behaviour of compounds (4) and (2) our previous treatment favoured model (*ii*) as an appropriate description. However, the magnetic data on the more extensive range of compounds now reported, plus the

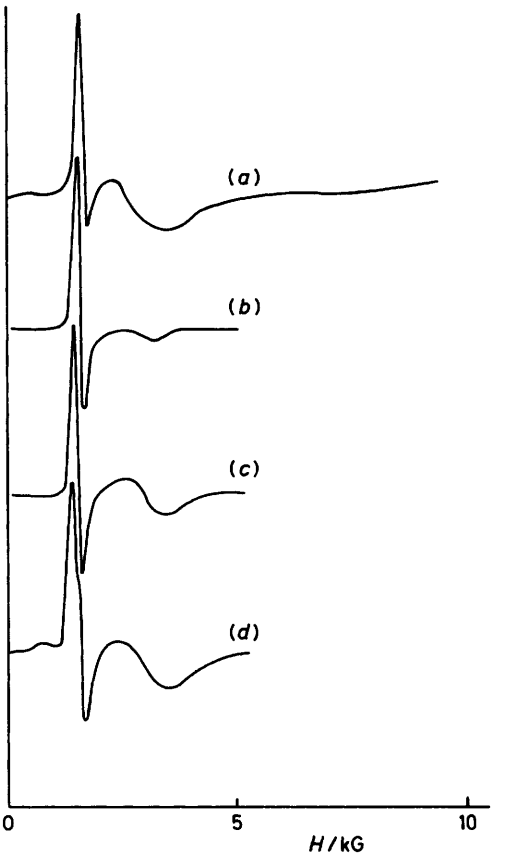

FIGURE 7 Frozen solution (10 K) e.s.r. spectrum of $[NEt_4]_3[Fe_6W_3S_8(SPh)_6(OMe)_3]$ (2), $\nu = 9.328$ GHz. (*a*) Experimental. Calculated spectra with $g_{\parallel} = 2.10$, $g_{\perp} = 2.20$, $D = 2.00$ cm^{-1}, $\delta H = 10$ G, $\Delta H = 200$ G, and $\delta\theta = 3°$: (*b*) $S = \frac{1}{2}$ only, $w_{\parallel} = 400$, $w_{\perp} = 150$ G; (*c*) superposition of $S = \frac{3}{2}$ in (*b*) plus $S = \frac{1}{2}$ with $w_{\parallel} = w_{\perp} = 1\,000$ G; (*d*) $|\beta J| = 0.012$ cm^{-1}, $E_a(S' = \frac{1}{2}) = E_b(S' = \frac{1}{2}) = 0.0$ cm^{-1}, $E_a(S' = \frac{3}{2}) = E_b(S' = \frac{3}{2}) = 4.0$ cm^{-1}. Linewidths for $S'_a = \frac{3}{2}$ coupled with $S'_b = \frac{1}{2}$ as in (*b*); for $S'_a = \frac{3}{2}$ coupled with $S'_b = \frac{1}{2}$ and *vice versa*, $w_{\parallel} = w_{\perp} = 1\,400$ G; for $S'_a = \frac{1}{2}$ coupled with $S'_b = \frac{1}{2}$, $w_{\parallel} = w_{\perp} = 1\,000$ G

crucial additional e.s.r. information on compound (2), require us to modify this description as detailed below. We found that not all of this more extensive data could be reproduced with either model (*ii*) or (*iii*) on the basis of independent cubane-like sub-units. However, allowing weak electronic exchange interactions between the sub-units has enabled us to reproduce (see below) the magnetic moment data of all four compounds, and the e.s.r. data of compound (2) very well. In this revised model the exchange interaction between the iron atoms, expressed in equation (1), within a sub-unit is still presumed to be the dominant perturbation.

Isotropic exchange interactions of the form used in equation (1) are the leading terms in a series expansion.[39-41] However, the use of an isotropic exchange interaction is only

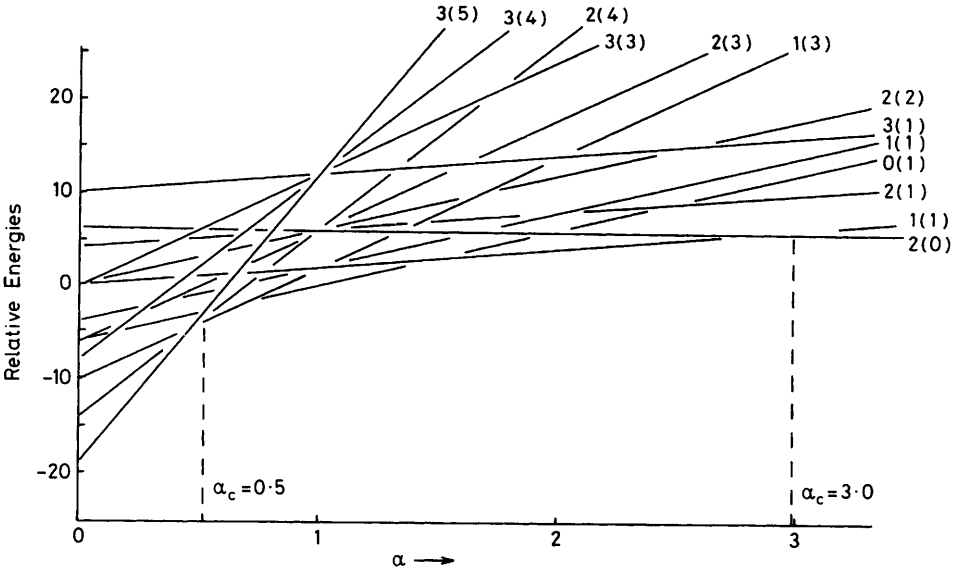

FIGURE 8 Relative energies of the lowest S' states as a function of α for model (*ii*). Energy levels are labelled as $S'(S^*)$

strictly justified when the ground states of the isolated interacting ions have no orbital angular momentum and when other orbital states are separated from it by energies which are large compared with the exchange and the spin-orbit interaction.[40,42,43] When these conditions are not satisfied more complex treatments are required (see for example refs. 40 and 43—47), although it is not always possible to choose between them and the isotropic exchange model when only average magnetic moments are available.[44,46-49] However, in the case of tetrahedral iron(II) the ground state has no orbital angular momentum associated with it in first order.[50] It has been observed that, apart from a small intramolecular antiferromagnetic interaction, the magnetic moment of $[NEt_4]_2[S_2MoS_2Fe(SPh)_2]$, which contains a distorted tetrahedral anion, is independent of temperature.[51] This is indicative of a ground state with no first-order orbital angular momentum. In addition, the absorption spectra of a number of distorted tetrahedral iron(II) complexes with sulphur donors have been interpreted in terms of orbital singlet ground states with excited states well separated from the ground state.[52] Thus the use of an isotropic exchange interaction in the present system would appear to be a reasonable first approximation [see equation (1)], where centres 1 and 2 are the iron atoms of like oxidation state which are initially coupled [53] (in terms of the exchange parameter αJ) to give a set of resultant spins S^*. These spins S^* are then coupled with the electronic spin, S_3, of the other iron atom to give a set of final resultant spins, S', for the sub-unit.

$$\mathscr{H}_{ex} = -2\alpha J\hat{S}_1.\hat{S}_2 - 2J\hat{S}^*.\hat{S}_3 \qquad (1)$$

The inter-sub-unit exchange, applied magnetic field, and zero-field splitting were considered as simultaneous perturbation *via* the Hamiltonian [see equation (2)].

$$\mathscr{H}_p = \sum_{i=a}^{b} \{g_\parallel\beta_e H_z\hat{S}'_z(i) + g_\perp\beta_e[H_x\hat{S}'_x(i) + H_y\hat{S}'_y(i)] + D[\hat{S}'^2_z(i) - \tfrac{1}{3}S'(S'+1)]\} - 2\beta J\hat{S}'_a.\hat{S}_b \qquad (2)$$

Equation (2) was applied to product spin functions $|S'(a)\ M_s(a),\ S'(b)M_s(b)\rangle$, the zero-order energies of which were taken as the sum of the energies $E_a(S'_a)$ of $S'(a)$ and $E_b(S'_b)$ of $S'(b)$ resulting from the application of equation (1). Also, all possible combinations of $S'(a)$ and $S'(b)$ which would lead to thermally occupied states were considered. The principal magnetic susceptibilities $\chi_\parallel$ and $\chi_\perp$ were calculated using equation (3) (N = Avogadro number), and $\bar{\chi}$, $\bar{\chi}_m$, and $\bar{\mu}_m$ from equations (4) and (5) respectively, where $j = z$ or x, and $\bar{\chi}_m$ is the average susceptibility of the whole cube-cluster dimer.

$$\chi_j = \frac{N\sum_i(-d\varepsilon_i/dH)_{exp}(^{-\varepsilon_{i/kT}})}{\sum_i \exp(-\varepsilon_i/kT)} \qquad (3)$$

$$\bar{\chi} = \tfrac{1}{3}(\chi_\parallel + 2\chi_\perp),\ = \bar{\chi}_m,\ \text{unless } \beta = 0 \text{ when } \bar{\chi}_m = 2\bar{\chi} \qquad (4)$$

$$\bar{\mu}_m = 2.828\ [\bar{\chi}_m(T-\theta)]^{\frac{1}{2}}\ \text{B.M.}^* \qquad (5)$$

The e.s.r. spectra were simulated using the technique reported in the preceding paper appropriately modified for the product basis functions. In performing the above calculations we assumed that the same set of values of the parameters $g_\parallel$, $g_\perp$, and D were applicable to each S' spin state.

Bulk Magnetic Properties.—The gross behaviour of $\bar{\mu}_m$ *versus* T for all four compounds suggests overall antiferromagnetic coupling, whilst the values of $\bar{\mu}_m$ at 4.2 K and *ca.* 2 K imply depopulation from a larger to a smaller but non-zero spin multiplet as the temperature is reduced. The application of equation (1) to models (*ii*) and (*iii*) shows for strong antiferromagnetic exchange within a sub-unit that there are critical values of α where two small paramagnetic S' levels become degenerate. These values are for model (*ii*) $\alpha_c = 3.00[S'(S^*) = 1(1)$ and $2(0)]$ and $\alpha_c = 0.50[S'(S^*) = 1(3)$ and $2(4)]$, and for model (*iii*) $\alpha_c = 1.750\ [S'(S^*) = \frac{1}{2}(2)$ and $\frac{3}{2}(1)]$ and $\alpha_c = 0.625\ [S'(S^*) = \frac{1}{2}(3)$ and $\frac{3}{2}(4)]$; see Figures 8 and 9. The effects on $\bar{\mu}_m$ of the various parameters in equations (1) and (2) are to some extent interdependent. However, some broad trends may be discerned. Close to a critical value of α the magnitude of $\bar{\mu}_m$, and its variation

* Throughout this paper: 1 B.M. = 0.927×10^{-23} A m^2; 1 G = 10^{-4} T.

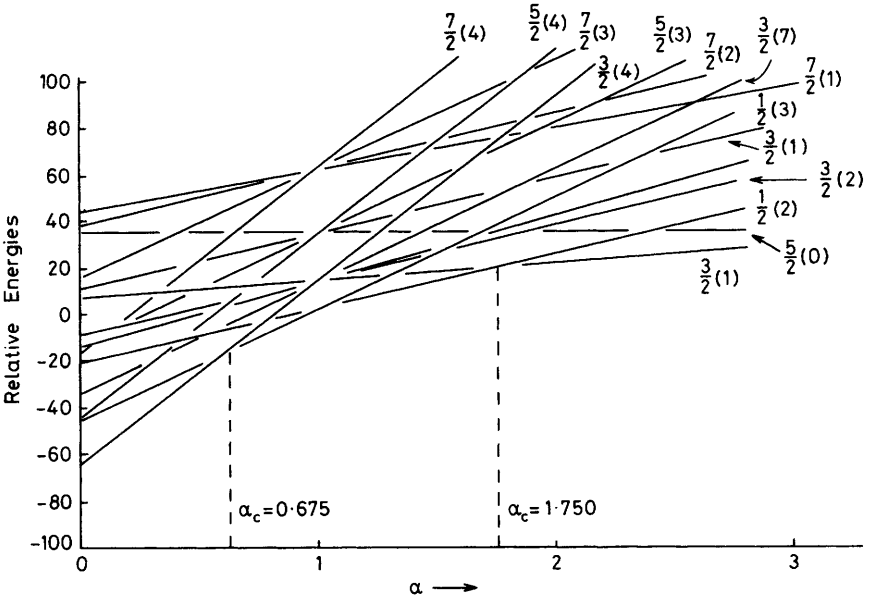

FIGURE 9 Relative energies of the lowest S' states as a function of α for model (*iii*). Energy levels are labelled as $S'(S^*)$

down to *ca.* 100 K, is determined largely by J and g [Figure 10(*a*) and (*b*)], whilst varying α for a fixed J affects $\bar{\mu}_m$ below this temperature [Figure 10(*c*)]. Because of thermal depopulation, the effects of D and β on $\bar{\mu}_m$ are noticeable only below *ca.* 20 K. Thus the variation of $\bar{\mu}_m$, with both temperature and applied magnetic field, is quite sensitive to changes in these parameters, see Figures 11 and 12. Our strategy for interpreting the magnetic data has been simultaneously to fit as closely as possible the value of $\bar{\mu}_m$ at room temperature, its temperature variation over the whole temperature range, and its variation with applied magnetic field at the two lowest temperatures.

Contrary to our earlier report that the magnetic properties of compounds (1) and (2) could only be fitted to model (*ii*), our extended examination reveals that the magnetic data can be fitted to both models (*ii*) and (*iii*). In each model however somewhat different values of the parameters, mainly $\bar{g}$ and α, are required. In addition the data can also be accounted for very well by allowing a small amount of inter-sub-unit coupling. Although this is not required to account for the magnetic data of these two compounds we find it necessary for an adequate interpretation of the e.s.r. spectrum of compound (2). Representative comparisons between the experimental and calculated magnetic data for (1) and (2) are given in Figures 1 and 2 and Tables 5 and 6, whilst the parameters for the calculation are summarised in Table 9.

The variation of $\bar{\mu}_m$ *versus* T for compound (3) differs

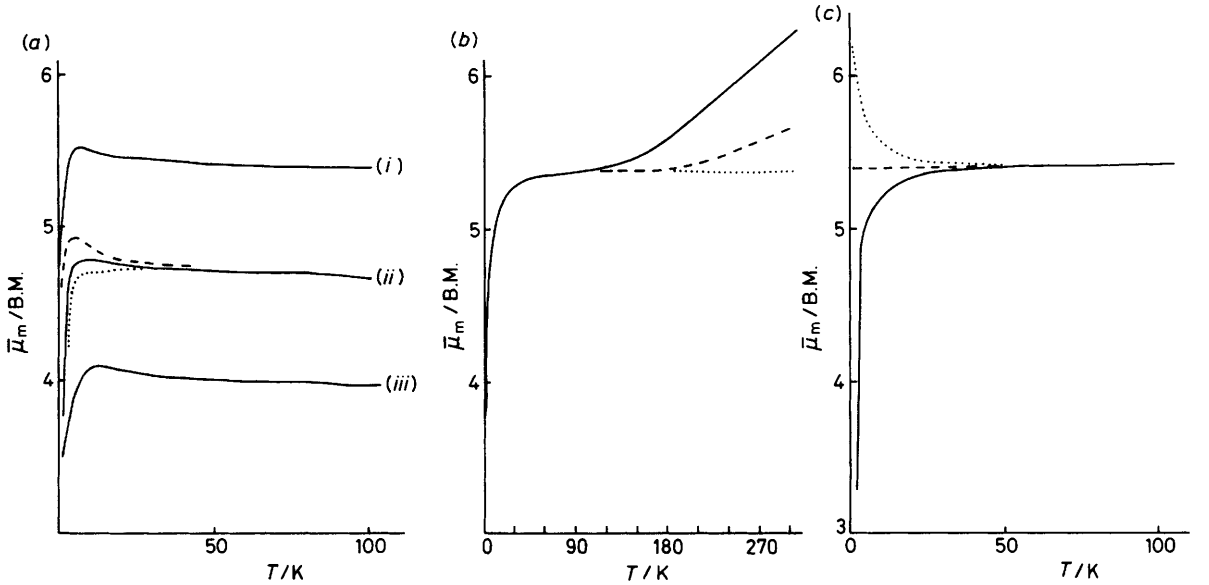

FIGURE 10 Calculated variation of $\bar{\mu}_m$ *versus* temperature: (*a*) $J = -120$ cm^{-1}, $\alpha = 0.6230$, $\beta = 0.005$, $D = 3.00$ cm^{-1}; with (*i*) $g_\parallel = g_\perp = 2.3$; (*ii*) $g_\parallel = g_\perp = 2.0$ (——), $g_\parallel = 1.8$, $g_\perp = 2.1$ (- - - -), $g_\parallel = 2.2$, $g_\perp = 1.9$ (· · · ·); (*iii*) $g_\parallel = g_\perp = 1.7$; (*b*) $\alpha = 0.627$, $\beta = 0.00$, $D = 0.00$ cm^{-1}, $g = g_\perp = 2.3$, $J = -80$ (——), -120 (- - - -), -200 cm^{-1} (· · · ·); (*c*) $J = -120$ cm^{-1}, $\beta = 0.00$, $D = 0.00$ cm^{-1}, $g_\parallel = g_\perp = 2.3$, $\alpha = 0.6270$ (——), 0.6250 (- - - -), 0.6230 (· · · ·)

markedly from that of the corresponding OMe-bridged species in that $\bar{\mu}_m$ passes through a maximum at 4.2 K, Figure 3. In addition $\bar{\mu}_m$ at *ca.* 2 K has a higher value and shows much more variation with magnetic field, see Table 7. We are able to account for these data using either model (*ii*) or (*iii*) *but only* if inter-sub-unit exchange is included. Representative comparisons of experimental and calculated $\bar{\mu}_m$ are given in Figure 3 and Table 7. The bulk susceptibility data do not enable us to distinguish between models (*ii*) and (*iii*).

The variation of $\bar{\mu}_m$ *versus* T for compound (4) is qualitatively similar to that of the two OMe-bridged compounds whilst the variation of $\bar{\mu}_m$ with H at low temperature is

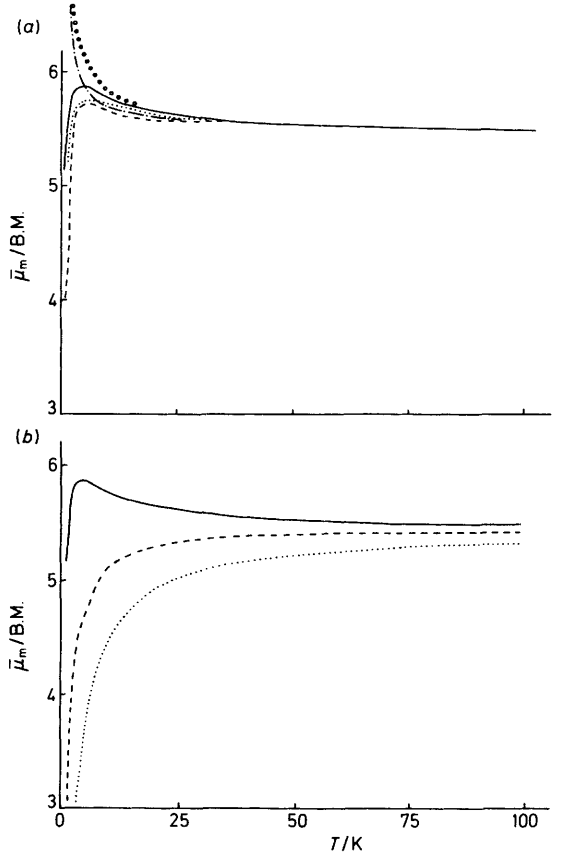

FIGURE 11 Calculated variation of $\bar{\mu}_m$ *versus* temperature for $J = -120$ cm^{-1}, $g_{\|} = 2.12$, $g_{\perp} = 2.42$, $\alpha = 0.6285$; (*a*) $\beta = -0.009$; $D = 0.00$ (– – –), $+1.25$ (——), -1.25 (· · ·), $+3.00$ (●), -3.00 cm^{-1} (– · – · –); (*b*) $D = +1.25$ cm^{-1}; $\beta = 0.000$ (– – –), -0.009 (——), $+0.009$ (· · ·)

intermediate between these latter species and the SPh-bridged molybdenum compound (3). Of the four compounds studied the worst reproduction of the magnetic data occurred for compound (4). In addition it was necessary to include a small value of θ in equation (5) in order to obtain satisfactory fits. The inclusion of θ was not necessary for the other three compounds. The requirement of a θ value for (4) may be a reflection of inter-cube-cluster dimer electronic exchange, but at present this is by no means certain. Once again the experimental data can be reasonably well reproduced by either model (*ii*) or (*iii*), see Figure 4 and Table 8.

E.S.R. Spectra.—The e.s.r. spectra of compounds (2)—(4) have been obtained from powders below *ca.* 20 K. The spectra of (3) and (4) were very broad and featureless at all temperatures studied, Figure 5. However, the e.s.r. spectrum of (2) was reasonably well resolved at 4.2 K, see Figure 6(*a*). Increasing the temperature reduced the intensity of the whole spectrum, and it was not observable above *ca.*

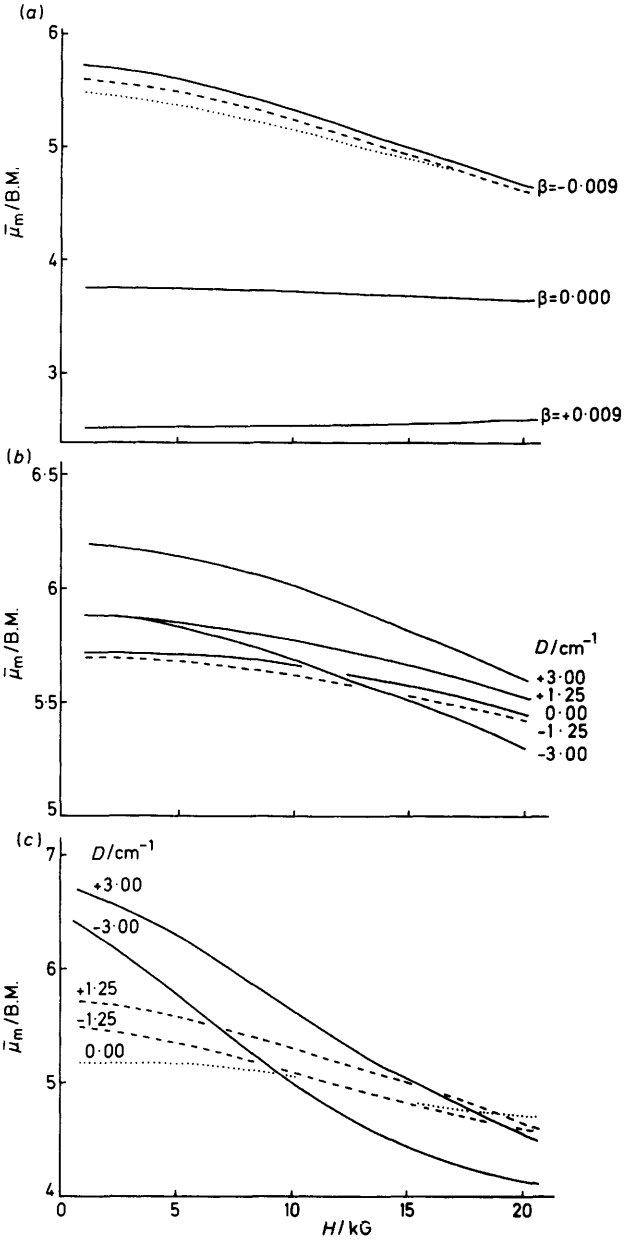

FIGURE 12 Calculated variation of $\bar{\mu}_m$ *versus* applied magnetic field for $J = -120$ cm^{-1}, $\alpha = 0.6285$; (*a*) $T = 4.18$ K, $D = +1.25$ cm^{-1}; $g_{\|} = 2.12$, $g_{\perp} = 2.42$ (——); $g_{\|} = g_{\perp} = 2.32$ (– – –); $g_{\|} = 2.52$, $g_{\perp} = 2.22$ (· · ·); (*b*) $T = 4.18$ K, $\beta = -0.009$, $g_{\|} = 2.12$, $g_{\perp} = 2.42$; (*c*) $T = 1.95$ K, $\beta = -0.009$, $g_{\|} = 2.12$, $g_{\perp} = 2.42$

25 K. The powder spectrum of compound (2) will now be discussed in some detail.

We have been unable to simulate the powder e.s.r. spectrum of (2), with respect to both relative intensities and position in terms of magnetic field, using only isolated spin

states, S', or superposition of spectra from a number of such isolated spin states. However, if we assume inter-sub-unit electronic exchange it is possible to obtain a very good simulation of the spectrum but *only* when model (*iii*) is used. In this compound there is good support for adopting model (*iii*). The values of J, α, and D are determined by the magnetic moment data. The e.s.r. spectrum at 4.2 K arises from only the lowest energy states and its simulation is not sensitive to J and α, nor is it sensitive to D because $D > h\nu$, where ν is the applied microwave frequency. However, the simulated e.s.r. spectrum is sensitive to g and β, and thus we have an independent check on these values. If the values of g and β required to fit the e.s.r. spectrum are used in the magnetic calculation we can obtain gratifyingly good agreement with the magnetic data at temperatures close to 4.2 K, see Table 10. However, the observed and calculated values of $\bar{\mu}_m$ diverge with increasing temperatures. This divergence could be accommodated by allowing J and/or g to be

TABLE 9

Parameters used in the magnetic calculation for models (*ii*) and (*iii*)

Compound	Model (*ii*)				Model (*iii*)					
parameter	(1)	(2)	(3)	(4)	(1a)	(1b)	(2a)	(2b)	(3)	(4)
$g_{\|\|}$	1.92	1.94	1.90	1.92	2.55	2.35	2.56	2.36	2.12	2.12
$g_{\perp}$	1.89	1.91	1.87	1.89	2.25	2.35	2.26	2.36	2.42	2.42
D/cm^{-1}	3.0	3.0	3.0	−5.0	2.0	2.0	2.0	2.0	1.25	4.0
J/cm^{-1}	−120	−120	−120	−120	−120	−120	−120	−120	−120	−120
α	2.975	2.970	2.978	2.975	0.6287	0.6291	0.6284	0.6288	0.6285	0.6288
β	−0.0004	−0.0006	−0.0051	−0.0005	−0.0006	−0.0014	+0.001	+0.0006	−0.009	−0.0022
θ/K	0	0	0	0	0	0	0	0	0	+0.5

the simulation we have confined our consideration to those spin states which will be significantly populated at the temperature of the experiments. From the calculation of the magnetic data this means that in the absence of inter-sub-unit coupling we need only consider $S' = \frac{1}{2}$ and $\frac{3}{2}$ on each sub-unit. The general form of the e.s.r. spectrum at 4.2 K is resonably well reproduced by only coupling $S'_a = \frac{1}{2}$ with $S'_b = \frac{3}{2}$ and *vice versa*, see Figure 6(*b*). The spectral profile can be improved by the inclusion of the other possible coupling schemes, *i.e.* $S'_a = \frac{1}{2}$ with $S'_b = \frac{1}{2}$, and $S'_a = \frac{3}{2}$ with $S'_b = \frac{3}{2}$, see Figure 6(*c*), although we found it necessary to use a greater molecular linewidth for these latter combinations.

The e.s.r. spectrum of compound (2) in frozen MeCN is much simpler than that of the powder, see Figure 7(*a*). This change between solid state and frozen solution is reminiscent of that observed for certain $[Fe_4S_4(SR)_4]^{3-}$ species.[12] By analogy with our simulations for FeMo cofactor, the apparent g values of *ca.* 4.4 and 2.1 may be indicative of the spectrum arising from an axially distorted $S = \frac{3}{2}$ species. In contrast to this we have been unable to simulate the observed spectral profile by assuming the presence of species with integral values of S. The general profile of the spectrum can be simulated on the basis of $S = \frac{3}{2}$, see Figure 7(*b*). However, in order to obtain the breadth of the feature at *ca.* 3 000 G we need to superimpose the spectrum of a $S = \frac{1}{2}$ species which has a much greater linewidth, see Figure 7(*c*). The change in the e.s.r. spectra between pure solid and frozen solution could be indicative of intramolecular interactions. However, it is possible to include coupling between the sub-units in the range $|\beta J| \leqslant 0.012$ cm^{-1} without significantly altering the form of the simulated spectrum, see Figure 7(*d*). Thus the frozen solution e.s.r. spectrum is still compatible with inter-sub-unit interaction as in the solid state, but to a smaller extent, although we cannot entirely rule out more extensive intermolecular interactions in the solid.

TABLE 10

Comparison of the observed magnetic data of $[NEt_4]_3[Fe_6W_2S_8(SPh)_6(OMe)_3]$ with that calculated using the e.s.r. parameters *

T/K	H/kG	$\bar{\mu}_m$/B.M. (Observed)	$\bar{\mu}_m$/B.M. (Calculated)
289.75	20.0	5.81	—
300.0	1.25	—	5.53
247.75	10.0	5.81	—
250.0	1.25	—	5.39
213.49	10.0	5.80	—
200.0	1.25	—	5.29
149.45	10.0	5.74	—
150.0	1.25	—	5.25
98.64	10.0	5.67	—
100.0	1.25	—	5.24
51.92	10.0	5.63	—
50.0	1.25	—	5.22
22.37	5.0	5.47	—
20.0	1.25	—	5.12
12.35	2.5	5.27	—
10.0	1.25	—	4.96
5.45	2.5	4.77	—
5.0	1.25	—	4.64
4.18	1.25	4.53	4.52
4.18	2.50	4.55	4.52
4.18	5.00	4.51	4.52
4.18	7.50	4.50	4.51
4.18	10.00	4.49	4.50
4.18	15.00	4.48	4.47
4.18	20.00	4.42	4.43
2.20	1.25	3.91	4.00
2.20	2.50	3.92	3.99
2.20	5.00	3.89	3.98
2.20	7.50	3.87	3.97
2.20	10.00	3.84	3.95
2.20	15.00	3.78	3.88
2.20	20.00	3.68	3.81

* Parameters used in the calculation: $J = -120$ cm^{-1}, $\alpha = 0.6282$, $\beta = 0.000\,25$, $g_{\|\|} = g_{\perp} = 2.25$, $D = 2.00$ cm^{-1}.

DISCUSSION

Compounds (1) *and* (2).—The magnetic moment data can be interpreted using both models (*ii*) and (*iii*). Within model (*iii*) either isotropic or axially symmetric g values may be employed and β can be either zero or non-zero. In contrast to this the e.s.r. spectrum of (2) at 4.2 K can only be simulated with model (*iii*), $\beta \neq 0$, and isotropic or nearly isotropic g values. Thus at least for

temperature dependent. Variations with temperature of these two parameters have either been observed [54] or suggested [55] in e.s.r. and magnetic studies on other transition metal complexes.

The value of αJ, the exchange coupling between the two Fe^{II} atoms in the preferred model, is *ca.* -75 cm^{-1}, approximately half the values of -158 and -148 cm^{-1} reported for the coupling between two Fe^{III} atoms in $[NEt_4]_2[Fe_2S_2Cl_2]$[34] and $[AsPh_4]_2[Fe_2S_2\{o\text{-}(SCH_2)_2C_6H_4\}_2]$.[56] In contrast to this the value of J (-120 cm^{-1}) for the coupling between the Fe^{III} atom and the resultants of the coupling between the two Fe^{II} atoms is larger than that reported for the range of values for $2Fe(Fd_{red.})$ (-70 to -110 cm^{-1}; $Fd_{red.}$ = a reduced ferredoxin).[57] This value of J is also larger than those from Xα-VB (Xα-valence bond) calculations on the model system $[Fe_2S_2(SH)_4]^{3-}$ (-76 to -82 cm^{-1}),[30] where the exchange is between single Fe^{II} and Fe^{III} ions. One interesting and perhaps unexpected feature of the present interpretation is the high individual and average g values required (>2.1). This is in marked contrast to the g values reported for many $[Fe_4S_4(SR)_4]^{3-}$ compounds,[37,58] and $Fd_{red.}$ proteins [59-63] where g is less than 2.00 and any one principal g value is usually $\leqslant 2.10$. One exception to this observation appears to be $[NMe_4]_3[Fe_4S_4(SC_6H_4Me)_4]$ in the solid state [58] where $\bar{g} = 2.7$ was required in order to obtain a reasonable simulation of the e.s.r. spectrum. The reason for these high g values is at present uncertain, but it is possible that they either represent inadequacies in the isotropic model [46] or that they may be due to admixtures of low energy charge-transfer states into the ground states *via* spin-orbit coupling. Such an admixture has been proposed for example to explain the $g_{\parallel}$ value >2.0 in $[CrOCl_4]^-$.[64]

Since the data for compound (2) seem to be only interpretable in terms of model (*iii*) we assume henceforth in our discussion that it also applied to the other compounds. On this basis the g value anisotropy for the best fit to compound (3) (Table 9) calls for special comment. The detailed temperature behaviour of $\bar{\mu}_m$ in this case is sensitive to the anisotropy in the g values, in contrast to the situation for compounds (1) and (2). If the g values are made isotropic, or given the reverse anisotropy, then the fit to the whole of the magnetic moment data deteriorates. The marked difference in g-value anisotropy between compounds (2) and (3) may be expected to be a reflection of significant structural differences between the two compounds. However, apart from the obvious differences in the bridging arrangement (OMe *versus* SPh) no such structural differences are observed.[1,3,10] In the absence of suitable crystals for single crystal anisotropy measurements the parameters in Table 9 represent the best interpretation of the available data on these compounds.

None of the currently known cube-cluster dimer compounds displays e.s.r. spectra exactly analogous to those of FeMo protein or FeMo cofactor from various sources. However, the comparison between the solid state and frozen solution e.s.r. spectra, together with the magnetic moment measurements on the synthetic compounds, and the interpretation of these data suggests that (*i*) the e.s.r. and magnetic moment are interpretable in terms of spin-coupled integral oxidation state iron ions, (*ii*) the e.s.r. spectra and magnetic properties are sensitive to the environment, and (*iii*) the form of the e.s.r. spectra may not necessarily be defined by considering only a single spin state.

We thank the S.R.C. for financial support.

[1/1873 *Received*, 2nd *December*, 1981]

REFERENCES

[1] G. Christou, C. D. Garner, F. E. Mabbs, and T. J. King, *J. Chem. Soc., Chem. Commun.*, 1978, 740.
[2] G. Christou, C. D. Garner, F. E. Mabbs, and M. G. B. Drew, *J. Chem. Soc., Chem. Commun.*, 1979, 91.
[3] S. R. Acott, G. Christou, C. D. Garner, F. E. Mabbs, T. J. King, and R. M. Miller, *Inorg. Chim. Acta*, 1979, **35**, L337.
[4] G. Christou, C. D. Garner, R. M. Miller, and T. J. King, *J. Inorg. Biochem.*, 1979, **11**, 349.
[5] T. E. Wolff, J. M. Berg, P. P. Power, K. O. Hodgson, and R. H. Holm, *J. Am. Chem. Soc.*, 1979, **101**, 4140.
[6] T. E. Wolff, J. M. Berg, P. P. Power, K. O. Hodgson, R. H. Holm, and R. B. Frankel, *J. Am. Chem. Soc.*, 1979, **101**, 5454.
[7] T. E. Wolff, J. M. Berg, P. P. Power, K. O. Hodgson, and R. H. Holm, *Inorg. Chem.*, 1980, **19**, 430.
[8] T. E. Wolff, P. P. Power, R. B. Frankel, and R. H. Holm, *J. Am. Chem. Soc.*, 1980, **102**, 4694.
[9] G. Christou and C. D. Garner, *J. Chem. Soc., Dalton Trans.*, 1980, 2354.
[10] G. Christou, C. D. Garner, T. J. King, C. E. Johnson, and J. D. Rush, *J. Chem. Soc., Chem. Commun.*, 1979, 503.
[11] G. Christou, C. D. Garner, R. M. Miller, C. E. Johnson, and J. D. Rush, *J. Chem. Soc., Dalton Trans.*, 1980, 2363.
[12] T. E. Wolff, J. M. Berg, C. Warwick, K. O. Hodgson, R. H. Holm, and R. B. Frankel, *J. Am. Chem. Soc.*, 1978, **100**, 4630.
[13] W. H. Armstrong and R. H. Holm, *J. Am. Chem. Soc.*, 1981, **103**, 6246.
[14] S. P. Cramer, K. O. Hodgson, W. O. Gillum, and L. E. Mortenson, *J. Am. Chem. Soc.*, 1978, **100**, 3398; S. P. Cramer, W. O. Gillum, K. O. Hodgson, L. E. Mortenson, E. I. Stiefel, J. R. Chisnell, W. J. Brill, and V. K. Shah, *ibid.*, p. 3814.
[15] G. Christou, D. Collison, C. D. Garner, F. E. Mabbs, and V. Petrouleas, *Inorg. Nucl. Chem. Lett.*, 1981, **17**, 137.
[16] D. B. Brown, Van. H. Crawford, J. W. Hall, and W. E. Hatfield, *J. Phys. Chem.*, 1977, **81**, 1303.
[17] R. S. Gall, C. T. W. Chu, and L. F. Dahl, *J. Am. Chem. Soc.*, 1974, **96**, 4019.
[18] T. Toan, W. P. Fehlhammer, and L. F. Dahl, *J. Am. Chem. Soc.*, 1977, **99**, 402.
[19] T. Toan, B. K. Teo, J. A. Ferguson, T. J. Meyer, and L. F. Dahl, *J. Am. Chem. Soc.*, 1977, **99**, 408.
[20] H. Wong, D. Sedney, W. M. Reiff, R. B. Frankel, T. J. Meyer, and D. Salmon, *Inorg. Chem.*, 1978, **17**, 194.
[21] B. A. Averill, T. Herskovitz, R. H. Holm, and J. A. Ibers, *J. Am. Chem. Soc.*, 1973, **95**, 3523.
[22] G. L. Simon and L. F. Dahl, *J. Am. Chem. Soc.*, 1973, **95**, 2164.
[23] A. S. Foust and L. F. Dahl, *J. Am. Chem. Soc.*, 1970, **92**, 7337.
[24] M. A. Neuman, Triah-Toan, and L. F. Dahl, *J. Am. Chem. Soc.*, 1972, **94**, 3383.
[25] R. A. Schunn, C. J. Fritchie, jun., and C. T. Prewitt, *Inorg. Chem.*, 1966, **5**, 892.
[26] C. H. Wei, G. R. Wikes, P. M. Treichel, and L. F. Dahl, *Inorg. Chem.*, 1966, **5**, 900.
[27] A. J. Thomson, *J. Chem. Soc., Dalton Trans.*, 1981, 1180; *Biochem. Soc. Trans.*, 1975, **3**, 468.
[28] C. Y. Yang, K. H. Johnson, R. H. Holm, and J. G. Norman, jun., *J. Am. Chem. Soc.*, 1975, **97**, 6596.
[29] A. P. Ginsberg, *J. Am. Chem. Soc.*, 1980, **102**, 111.
[30] J. G. Norman, jun., P. B. Ryan, and L. Noodleman, *J. Am. Chem. Soc.*, 1980, **102**, 4279.
[31] M. Cerdinio, R. H. Wang, R. Rawlings, and H. B. Gray, *J. Am. Chem. Soc.*, 1974, **96**, 6534.

[32] W. D. Phillips, M. Poe, C. C. McDonald, and R. G. Bartsch, *Proc. Natl. Acad. Sci. USA*, 1970, **67**, 682.
[33] M. Poe, W. D. Phillips, C. C. McDonald, and W. Lovenberg, *Proc. Natl. Acad. Sci. USA*, 1970, **65**, 797.
[34] G. B. Wong, M. A. Bobrik, and R. H. Holm, *Inorg. Chem.*, 1978, **17**, 578.
[35] M. A. Bobrik, E. J. Laskowski, R. W. Johnson, W. O. Gillum, J. M. Berg, K. O. Hodgson, and R. H. Holm, *Inorg. Chem.*, 1978, **17**, 1402.
[36] E. J. Laskowski, R. B. Frankel, W. O. Gillum, G. C. Papaefthymiou, J. Renaud, J. A. Ibers, and R. H. Holm, *J. Am. Chem. Soc.*, 1978, **100**, 5322.
[37] E. J. Laskowski, J. G. Reynolds, R. B. Frankel, S. Foner, G. C. Papaefthymiou, and R. H. Holm, *J. Am. Chem. Soc.*, 1979, **101**, 6562.
[38] G. C. Papaefthymiou, R. B. Frankel, S. Foner, E. J. Laskowski, and R. H. Holm, *J. Phys. Colloq.* (*Fr.*), 1980, 41, C1-493.
[39] K. W. H. Stevens, *Rev. Mod. Phys.*, 1954, **25**, 166.
[40] A. Abragam and B. Bleaney, 'Electron Paramagnetic Resonance of Transition Metal Ions,' Clarendon Press, Oxford, 1970.
[41] O. Kahn, *Mol. Phys.*, 1075, **29**, 1039.
[42] J. W. Culvahouse and D. P. Schinke, *Phys. Rev.*, 1969, **187**, 671.
[43] M. E. Lines, *J. Chem. Phys.*, 1971, **55**, 2977.
[44] M. E. Lines, A. P. Ginsberg, R. L. Martin, and R. C. Sherwood, *J. Chem. Phys.*, 1972, **57**, 1.
[45] A. P. Ginsberg, M. E. Lines, K. D. Karlin, S. J. Lippard, and F. J. DiSalvo, *J. Am. Chem. Soc.*, 1976, **98**, 6958.
[46] P. W. Ball and A. B. Blake, *J. Chem. Soc., Dalton Trans.*, 1974, 852.
[47] P. D. W. Boyd, M. Gerloch, J. H. Harding, and R. G. Woolley, *Proc. R. Soc. London, Ser. A*, 1978, **360**, 161; P. D. W. Boyd, J. E. Davies, and M. Gerloch, *ibid.*, p. 191; M. Gerloch and J. H. Harding, *ibid.*, p. 211.
[48] V. T. Kalinnikov, Y. V. Rakitin, and W. E. Hatfield, *Inorg. Chim. Acta*, 1978, **31**, 1.
[49] D. M. Duggan and D. N. Hendrickson, *Inorg. Chem.*, 1975, **14**, 1944.
[50] D. Polder, *Physica*, 1942, **9**, 709; B. N. Figgis, *J. Chem. Soc.*, 1965, 4887; B. N. Figgis and J. Lewis, *Prog. Inorg. Chem.*, 1964, **6**, 37.
[51] R. H. Tieckelmann, H. C. Silvis, T. A. Kent, B. H. Huynh, J. V. Waszczak, Boon-Keng Teo, and B. A. Averill, *J. Am. Chem. Soc.*, 1980, **102**, 5550.
[52] R. W. Lane, J. A. Ibers, R. B. Frankel, G. C. Papaefthymiou, and R. H. Holm, *J. Am. Chem. Soc.*, 1977, **99**, 84; D. Concouvanis, D. Swenson, N. C. Baenziger, C. Murphy, D. G. Holah, N. Sfarnas, A. Simopoulos, and A. Kostikas, *J. Am. Chem. Soc.*, 1981, **103**, 3350.
[53] F. E. Mabbs and D. J. Machin, 'Magnetism and Transition Metal Complexes,' Chapman and Hall, London, 1973, ch. 7.
[54] See for example, F. E. Mabbs and J. K. Porter, *J. Inorg. Nucl. Chem.*, 1973, **35**, 3219.
[55] See for example, E. J. Laskowski, R. B. Frankel, W. O. Gillum, G. C. Papaefthymiou, J. Renaud, J. A. Ibers, and R. H. Holm, *J. Am. Chem. Soc.*, 1978, **100**, 5322; J. Lewis, F. E. Mabbs, and H. Weigold, *J. Chem. Soc. A*, 1968, 1699.
[56] W. O. Gillum, R. B. Frankel, S. Foner, and R. H. Holm, *Inorg. Chem.*, 1976, **15**, 1095.
[57] H. Blum, F. Adar, J. C. Salerno, and J. S. Leigh, jun., *Biochem. Biophys. Res. Commun.*, 1977, **77**, 650.
[58] D. Collison and F. E. Mabbs, *J. Chem. Soc., Dalton Trans.*, preceding paper.
[59] R. Cammack, *Biochem. Biophys. Res. Commun.*, 1973, **54**, 548; *J. Phys.* (*Paris*), 1976, **37**, C6-137; *Biochem. Soc. Trans.*, 1975, **3**, 482.
[60] N. A. Stombaugh, R. H. Burris, and W. H. Orme-Johnson, *J. Biol. Chem.*, 1973, **248**, 7951.
[61] R. N. Mullinger, R. Cammack, K. K. Rao, D. O. Hall, D. P. E. Dickson, C. E. Johnson, J. D. Rush, and A. Simopoulos, *Biochem. J.*, 1975, **151**, 75.
[62] R. Matthews, S. Charlton, R. H. Sands, and G. Palmer, *J. Biol. Chem.*, 1974, **249**, 4326.
[63] R. E. Anderson, G. Anger, L. Peterson, A. Ehrenberg, R. Cammack, D. O. Hall, R. Mullinger, and K. K. Rao, *Biochim. Biophys. Acta*, 1975, **376**, 63.
[64] C. D. Garner, I. H. Hillier, F. E. Mabbs, C. Taylor, and M. F. Guest, *J. Chem. Soc., Dalton Trans.*, 1976, 2258; C. D. Garner, J. Kendrick, P. Lambert, F. E. Mabbs, and I. H. Hillier, *Inorg. Chem.*, 1976, **15**, 1287.